Condensed Matter Physics 2009, Vol. 12, No 2, pp. 239–248

CONDENSED MATTER PHYSICS

Excitons into one-axis crystals of zinc phosphide (Zn_3P_2)

D.M.Stepanchikov*, G.P.Chuiko

Kherson national technical university, department of general and applied physics, research laboratory of the theory of solids, Berislavske shosse, 24, 73008, Kherson, Ukraine

Received May 18, 2008, in final form May 18, 2009

Theoretical study of excitons spectra is offered in this report as for Zn_3P_2 crystals. Spectra are got in the zero approach of the theory of perturbations with consideration of both the anisotropy of the dispersion law and the selection rules. The existence of two exciton series was found, which corresponds to two valence bands (hh, lh) and the conductivity band (c). It is noteworthy that anisotropy of the dispersion law plus the existence of crystalline packets (layers) normal to the main optical axis, both will permit the consideration of two-dimensional excitons too. The high temperature displaying of these $2D$-exciton effects is not eliminated even into bulk crystals. The calculated values of the binding energies as well as the oscillator's strength for the optical transitions are given for a volume ($3D$) and for two-dimensional ($2D$) excitons. The model of energy exciton transitions and four-level scheme of stimulated exciton radiation for receiving laser effect are offered.

Key words: *excitons, zinc phosphide, one-axis crystals*

PACS: *71.18.+y*

1. Introduction

The electronic properties of highly anisotropic systems such as confined systems or layered crystals have received much attention due, among other reasons, to the possibility of growing high-quality nanostructures with prescribed configurations, allowing the control of physical properties such as carrier densities, band gaps and bandwidths, and even dimensionality. On the other hand, excitons are important excitations that strongly affect electronic and optical properties of bulk and low-dimensional solids.

In this respect, the II–V compound semiconductors are of interest for several reasons. Firstly, these are possible applications and secondly come the band structure parameters and layered crystalline structures [1–11]. Now II–V compounds have come to show strong promise of constituting the next generation of electronic materials. Among these, zinc phosphide (Zn_3P_2), the constituent elements of which are known to be present in abundant deposits near the surface of the earth, is drawing particularly strong attention as a material which it is hoped will make it possible to produce highly efficient solar cells, sensors, lasers and the like at low cost [12–15].

Due to the large excitonic radii of II–V materials, they are expected to exhibit pronounced size quantization effects. The electrons in such a semiconductor will become confined in crystals much larger than for the analogous II–VI or III–V semiconductors. However, compared with the significant progress in bulk and low-dimensional II–VI and III–V semiconductors, research on II–V semiconductors has been lingering far behind due to the lack of appropriate and generalized synthetic methodologies. Now this problem of producing II–V compound semiconductors (including nanoscales) has been substantially decided [16–20]. Therefore, theoretical studies of the features of band structure of II–V materials once again become an urgent problem.

The main features and the quality of semiconductor devices are determined by the edge of optical absorption of the basic material. Excitons may substantially affect the form of this edge, particular through the appearance of discrete levels inside the band gap. Knowledge of the levels

*E-mail: step_75@mail.ru

located within the energy gap is important both for the potential applications and for the qualitative evaluation of a material. For the practical application of the II–V compound semiconductors, however, it is necessary to study the problems posed by the fact that they are defect semiconductors having several vacancies in their unit cells. As a result, these semiconductors include numerous defect deep levels attributed to the deficiency of atoms [4,21,22]. The interaction between excitons and such defect levels can be a reason to exciton recombination. In this case, the creation of multiple-exciton complexes is very possible too. Reduction of system dimensionality sharply intensifies these effects. However, the exciton states in II–V semiconductors have not been extensively examined yet. For Zn_3P_2 crystals, the exciton spectrum calculations have not been described so far.

This paper presents a theoretical study with fresh manner of modelling the exciton spectra as for Zn_3P_2 crystals. For the first time the exciton binding energy and oscillator strength of exciton transitions are calculated. Besides that, the layered crystalline structure, anisotropy of dispersion law, possible two-dimensional exciton spectrum and selection rules are taken into account. The electron, hole and exciton effective masses are calculated in the framework of generalized Kildal band model. The model of Wannier-Mott excitons is used for exciton spectrum calculations. The four-level scheme of possible stimulated exciton radiation at low temperature is received.

2. Crystalline structure

Zn_3P_2 is one of four crystallographically similar semiconductors of the type $A_3^{II}B_2^{V}$. The others are Cd_3P_2, Zn_3As_2 and Cd_3As_2. Materials with a common chemical formula $A_3^{II}B_2^{V}$ differ by the variety of crystalline forms. They have anion sublattices in close proximity to the standard FCC packing. Their cations occupy only three quarters of tetrahedral emptiness among anions. Thus, their cation sublattices contain exactly a quarter of vacancies, which may be recognized even as stoichiometric. Different ways of allocation of these vacancies determine the key features of all crystalline forms. Fully disordered high-temperature phosphide β-phases have, for instance, a cubic symmetry. The partly ordered crystals (α''-phases) demonstrate a tetragonal symmetry.

Phase transition $\beta \to \alpha''$ for Zn_3P_2 crystals occurs at $T = 1118$ K [23,24]. A positional order arises up in this transition, and typical energy of the positional ordering is 0.078 eV [24]. Herein below we should like to examine the partly ordered low-temperature tetragonal α''-phases. Zinc vacancy levels were suggested as the origin of the 0.19 eV acceptor (singly ionized) and the 0.29 eV acceptor (doubly ionized) [21].

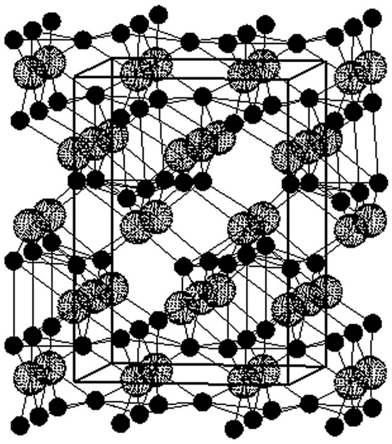

Figure 1. A general view of the crystal structure of Zn_3P_2 (bigger spheres present P, smaller spheres – Zn atoms).

The crystal structure of the tetragonal modification of Zn_3P_2 (see figure 1) is a primitive tetragonal lattice with a unit cell containing 16 P atoms and 24 Zn atoms. The space group is $P4_2/\mathrm{nmc}\left(D_{4h}^{15}\right)$ with the following parameters of a unit cell: $a = b = 8.0889$ Å and $c = 11.4069$ Å [1–6].

The presence of a quarter of vacant sites into the cation sublattice is a “logo” of these crystalline structures. Each cation atom (Zn) has the tetrahedral coordination with their nearest neighbors, i.e. with four phosphorus atoms, whereas those surrounded by cation atoms are located only at six of the eight corners of a coordinating cube. Two vacant sites are located either at diagonal corners of a cubic face or at the opposite spots of a space cubic diagonal [1–6,24].

An examination of figure 1 shows that there are two kinds of phosphorus layers and four of cations. The four cation layers differ in the positions of cation vacancies [1]. Other authors consider this structure as a simplest polytype consisting of two layered packets normal to the main axis.

In the extended elementary cell ($a\sqrt{2}\times a\sqrt{2}\times$c) the crystalline structure of the α''-modification can be presented as the sequence of two non-equivalent layered packets alternated along the main axis – X, Y. Every packet consists of four atomic layers. The packet contains two different layers of the close packed anions (α, β) alternated by two layers of cations (A, B), so that: $X = \alpha A\beta B$. Furthermore, the packet X transforms to the packet Y, and vice versa, by partial translations $\left(a\sqrt{2}+c\right)/2$ in the coordinate system of the extended elementary cell. The atomic layers, as well as the layered packets, are normal towards the main axis of crystal [24].

Such structures, more tightly filled with the metal atoms, should enhance the interaction between them and increase the metallic contribution to the chemical bond in comparison with III–V and II–VI compounds. The average number of electrons per bond is 4/3, and it is palpable less than standard digit of 2 electrons per bond as for conventional semiconductors with the tetrahedral coordination. Such relative deficiency of bonding electrons realizes itself in a descent of equilibrium bond lengths. Most of the bond lengths (56 from 96) remain close to the sum of covalent radii in the tetrahedral coordination (2.41 Å), but the remaining 40 bond lengths displace themselves below the sum of ionic radii (2.86 Å). The value of fractional ionicity is $0.17 \div 0.19$. The chemical bond for Zn_3P_2 is therefore a complex ionic-metallic-covalent bond [2,5–7,11]. It is also possible to think that forces of bonds are different: they may be much stronger into the layered packets, than between them.

3. Band model

The dispersion law for $A_3^{II}B_2^{V}$ semiconductors within the framework of model [8,25] has such a form nearby the point $\mathbf{k} = 0$ and with spherical coordinates (k, θ, φ):

$$(\Gamma(E) - (Pk)^2(f_1(E)\sin^2(\theta) + f_2(E)\cos^2(\theta))^2 - (Pk)^2 f_3^2(E)\sin^2(\theta) = 0, \tag{1}$$

$$\Gamma(E) = E\,(E - E_{\mathrm{g}})\left(\left(E + \frac{2\Delta}{3}\right)\left(E + \delta + \frac{\Delta}{3}\right) - \frac{2\Delta^2}{9\eta^2}\right), \tag{2}$$

$$f_1(E) = \left(E + \frac{\Delta}{3}\right)\left(E + \delta + \frac{\Delta}{3}\right) - \frac{\Delta^2}{9\eta^2}, \tag{3}$$

$$f_2(E) = E\left(E + \frac{2\Delta}{3}\right)\eta^{-4}, \tag{4}$$

$$f_3(E) = \frac{2}{3\eta}E\Delta d. \tag{5}$$

Thereto: (E_{g}, Δ, P) – are three well-known Kane's parameters (the energy gap, the spin-splitting parameter and the matrix element of the impulse); δ – is the known parameter of the crystal field; d – is another parameter of the crystal field, which describes the absence of symmetry center; $\eta = c/(a\sqrt{2})$ – is the scalar factor taking into account the deformation of the lattice. The numerical values of band parameters are presented in table 1 as if deserving the trust. It may be pointed out that a dispersion law similar to (1) has been also found in wurtzite-type bulk crystals and in some two-dimensional systems (e.g. heterojunctions and inversion layers) [27].

Hamiltonian (1) describes a surface of rotation around the main crystalline axis. This Hamiltonian is obviously of the fourth order, that is for k and has quite evident decomposition into the product of two factors P_+ and P_- [25]:

$$P_+\,(k, E, \theta)\,P_-\,(k, E, \theta) = 0, \tag{6}$$

where

$$P_\pm\,(k, E, \theta) = \Gamma(E) - (Pk)^2(f_1(E)\sin^2(\theta) + f_2(E)\cos^2(\theta) \pm Pkf_3(E)\sin(\theta). \tag{7}$$

On the other hand, it might be simplified to the two identical surfaces, both of second order, under the additional condition: $d = 0; f_3(E) = 0 \Rightarrow P_+ = P_-$. Physically, this condition means the presence of the symmetry center into a crystal [26]. This is just the case for $P4_2/\mathrm{nmc}$ (D_{4h}^{15})

modifications of $A_3^{II}B_2^{V}$ compounds. Each energy level should be twice degenerated according to this. Obviously, we deal with the well-known Kramer's degeneration at this rate. Therefore, by using expressions (2-5) the equations (7) become as follows:

$$\begin{aligned} P_{\pm}(k,E,\theta) \;\; = \;\; & \frac{E}{9\eta^4}\left[(E-E_{\rm g})\,\eta^2\left(-2\Delta^2+(3\,(E+\delta)+\Delta)\,(3E+2\Delta)\,\eta^2\right)\right.\\ & \left.+3k^2P^2\left(-(3E+2\Delta)\cos^2(\theta)-(3\,(E+\delta)+2\Delta)\,\eta^4\sin^2(\theta)\right)\right]=0. \qquad (8) \end{aligned}$$

Dispersion equation (8) has four non-identical solutions describing the conductivity band (c), the heavy holes band (hh), the light holes (lh) and spin-orbital split bands (so), respectively (see figure 2). These direct solutions might be obtained even in radicals, although proper expressions are quite cumbersome and unbelievably long. But in a special case ($\mathbf{k_0}=0$, Γ-point, band extrema) we get simple roots

$$E_0^c=E_{\rm g};\,E_0^{\rm hh}=0;\,E_0^{\rm lh,so}=-\frac{3\eta\,(\delta+\Delta)\mp\sqrt{9\delta^2\eta^2-6\delta\Delta\eta^2+\Delta^2\,(8+\eta^2)}}{6\eta}\,. \qquad (9)$$

In the last equation the sign "–" and "+" correspond to lh-band and so-band, respectively. The top of the hh-band is selected as the zero energy coordinates. Two of the three valence bands (hh and lh) are somewhat narrow within this model.

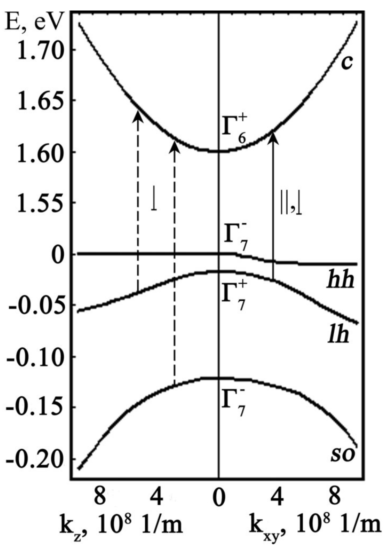

Figure 2. Energy band structure of Zn_3P_2 at the Γ point.

The knowledge of selection rules is also necessary for any interpretation of the optical band-to-band transitions and for classification of the exciton states. The selection rules for Zn_3P_2 depend on the direction of polarization vector ($\mathbf{e}_p$) of the light. As it is shown in [5], at the Γ point there were indicated such "allowed" transitions (see figure 2): $\Gamma_i^{\pm}\to\Gamma_j^{\pm}$ for the light polarized both perpendicular ($\mathbf{e}_p\perp$c) and parallel ($\mathbf{e}_p\,\|$c) to the main crystalline c-axis, and $\Gamma_i^{\pm}\to\Gamma_j^{\mp}$ for the light polarized perpendicular to the c-axis only ($\mathbf{e}_p\perp$c; i, j = 6.7). "Forbidden" transitions ($\Gamma_i^{\pm}\to\Gamma_j^{\mp}$ in ($\mathbf{e}_p\,\|$c) polarization conditions) are unallowable exactly in $\mathbf{k_0}=0$ only. Near the $\mathbf{k_0}=0$ point these transitions are allowed. Only s-excitons are capable of being generated for the"allowed" transitions, whereas just p-excitons are capable of being generated for the "forbidden" transitions [28]. In ($\mathbf{e}_p\perp$c) polarization conditions, both longitudinal and transversal excitons are generated. However, the longitudinal excitons are not generated in ($\mathbf{e}_p\,\|$c) polarization conditions [29]. As we know, the generation of the transversal excitons is more probable in layered crystals. Therefore, below we considered transversal excitons only.

Let us rewrite the simplified equation (8) with Cartesian coordinates and in accordance with the above supposition:

$$\left(k_x^2+k_y^2\right)P^2f_1(E)+k_z^2P^2f_2(E)-\Gamma(E)=0. \qquad (10)$$

Certainly, the equation (10) describes a surface of the second order in the $\mathbf{k}$-space. Therefore, effective masses associate themselves with two semi-axes of this surface.

$$m_{\perp} \;=\; \frac{\hbar^2\Gamma(E)}{2(E-E_0)P^2f_1(E)}=\frac{\hbar^2\eta^2\,(E-E_{\rm g})\left((3\,(E+\delta)+\Delta)\,(3E+2\Delta)\,\eta^2-2\Delta^2\right)}{6P^2\,(E-E_0)\,(3E+2\Delta)}\,, \qquad (11)$$

$$m_{\|} \;=\; \frac{\hbar^2\Gamma(E)}{2(E-E_0)P^2f_2(E)}=\frac{\hbar^2\eta^2\,(E-E_{\rm g})\left((3\,(E+\delta)+\Delta)\,(3E+2\Delta)\,\eta^2-2\Delta^2\right)}{2P^2\,(E-E_0)\,((3E+\Delta)\,(3\,(E+\delta)+\Delta)\,\eta^2-\Delta^2)}\,. \qquad (12)$$

Therein E_0 is the energy of the corresponding band extreme at the Γ point (see equations (9). The band energy values E were taken close to extremes E_0 for identical values of a wave-vector $\mathbf{k} \to \mathbf{k_0}$ and two polar angles $\theta = \frac{\pi}{2}; 0$. It corresponds to equations of the transversal (11) and longitudinal (12) effective masses respectively. The band parameters and the calculated values of energies E_0, E and the effective masses $m_\perp, m_\parallel$ for actual bands are shown in table 1.

Table 1. The main band parameters of Zn_3P_2.

E_{g}, eV [1]	Δ, eV [5]	P, eVm [9]	δ, eV [5]	η
1.60	0.11	$4.7 \cdot 10^{-10}$	0.03	0.9971
parameter	c-band	hh-band	lh-band	so-band
E_0, eV	1.60	0	-$1.78 \cdot 10^{-2}$	-$1.22 \cdot 10^{-1}$
$E\,(\theta = \pi/2)$, eV	1.61	-$6.75 \cdot 10^{-4}$	-$1.80 \cdot 10^{-2}$	-$1.223 \cdot 10^{-1}$
$E\,(\theta = 0)$, eV	1.61	-$3.18 \cdot 10^{-4}$	-$1.81 \cdot 10^{-2}$	-$1.230 \cdot 10^{-1}$
$m_\perp/m_0$	0.28	-0.57	-1.18	-1.11
$m_\parallel/m_0$	0.29	25.95	-0.53	-0.63

4. Calculations

Let us consider the model of Wannier-Mott excitons. Participation of phonons in exciton generation is of little probability due to a direct band structure of Zn_3P_2. So, the exciton-phonon interaction is not considered below. Moreover, the exchange interaction and polariton effects are not considered herewith too. It is known that an exciton spectrum and the wave functions are determined from the Schrödinger equation. With spherical coordinates, this equation may be written down for one-axis crystals as [30]:

$$\left[-\nabla^2 - \frac{2}{r}\frac{1}{\sqrt{1-\alpha\cos^2\theta}} - E\right]\Psi\left(r,\theta,\varphi\right) = 0, \tag{13}$$

where parameter of anisotropy α is calculated from the relation

$$\alpha = 1 - \frac{\varepsilon_\perp \mu_\perp}{\varepsilon_\parallel \mu_\parallel}\,. \tag{14}$$

The physical sense has a module of the parameter of anisotropy. Two marginal cases are the maximal anisotropy if $\mid \alpha \mid \longrightarrow 1$ and the full isotropy if $\mid \alpha \mid \longrightarrow 0$.

Equation (13) is written in the atomic units of length $a_{\mathrm{B}\perp} = 4\pi\varepsilon_0\hbar^2\sqrt{\varepsilon_\parallel\varepsilon_\perp}/(\mu_\perp e^2)$ (effective Bohr radius), energy $E_{\mathrm{B}} = \mu_\perp e^4/\left(32\hbar^2\pi^2\varepsilon_0^2\varepsilon_\perp\varepsilon_\parallel\right)$ (effective Rydberg), $\mu_\perp = m_\perp^{\mathrm{e}} m_\perp^{\mathrm{h}}/(m_\perp^{\mathrm{e}} + m_\perp^{\mathrm{h}})$; $\mu_\parallel = m_\parallel^{\mathrm{e}} m_\parallel^{\mathrm{h}}/(m_\parallel^{\mathrm{e}} + m_\parallel^{\mathrm{h}})$ are the transversal and longitudinal effective masses of the exciton respectively; $m_\perp^{\mathrm{e}}; m_\parallel^{\mathrm{e}}; m_\perp^{\mathrm{h}}; m_\parallel^{\mathrm{h}}$ are the transversal and longitudinal effective masses of electrons (e) and holes (h) (see equations 11, 12); $\varepsilon_\perp; \varepsilon_\parallel$ are two dielectric constants normal to the main crystalline c-axis and along that, respectively. In our calculation there was accepted a simple supposition: $\varepsilon_\parallel = \varepsilon_{\parallel\infty} = n_{\parallel\infty}^2$, $\varepsilon_\perp = \varepsilon_{\perp\infty} = n_{\perp\infty}^2$ and $\varepsilon_\perp$=15.13 [32]. From relation $\Delta n_\infty = n_{\parallel\infty} - n_{\perp\infty} = 0.02$ [5] the longitudinal dielectric constant was found $\varepsilon_\parallel$=15.28.

In a space of q dimension (qD) the Laplace operator is [31]

$$\nabla^2 = \frac{1}{r^{q-1}}\frac{\partial}{\partial r}\left(r^{q-1}\frac{\partial}{\partial r}\right) + \frac{1}{r^2}\left(\frac{1}{\sin^{q-2}\theta}\frac{\partial}{\partial\theta}\sin^{q-2}\theta + \frac{1}{\sin^2\theta}\frac{\partial^2}{\partial\varphi^2}\right). \tag{15}$$

It is possible to use the perturbation methods for solving the equation (13). This way we get the exciton energy spectrum in the zero-order approximation.

$$E_{nlm}^{qD}(\alpha) = E_{\mathrm{g}} - E_b^{qD} = E_{\mathrm{g}} - \frac{E_{\mathrm{B}}}{\left(n + \frac{q-3}{2}\right)^2} Z_{lm}^2(\alpha), \tag{16}$$

where E_b^{qD} is the binding energy of an exciton; n is the main quantum number; $Z_{lm}(\alpha)$ is an efficient charge depending on anisotropy.

We consider the s-type (thus $l = 0$; $m = 0$) and p-type (thus $l = 1$; $m = 0, \pm 1$) states of an exciton. Under these conditions $Z_{lm}(\alpha)$ may be written as [30]:

$$Z_{0.0}(\alpha) = I_1(\alpha), \tag{17}$$

$$Z_{1.0}(\alpha) = \frac{3}{2}\left[\frac{1}{\alpha} I_1(\alpha) - I_2(\alpha)\right], \tag{18}$$

$$Z_{1,\pm 1}(\alpha) = \frac{3}{2}\left[\left(1 - \frac{1}{2\alpha}\right) I_1(\alpha) + \frac{1}{2} I_2(\alpha)\right]. \tag{19}$$

Here the coefficients $I_1(\alpha)$, $I_2(\alpha)$ are determined by piecewise-continuous expressions:

$$I_1(\alpha) = \begin{cases} \frac{1}{\sqrt{\alpha}} \arcsin(\alpha), & \alpha > 0, \\ 1, & \alpha = 1, \\ \frac{1}{\sqrt{|\alpha|}} \mathrm{Arsh}\left(\sqrt{|\alpha|}\right), & \alpha < 0, \end{cases} \tag{20}$$

$$I_2(\alpha) = \frac{\sqrt{1-\alpha}}{\alpha}. \tag{21}$$

Free excitons are capable of generating themselves owing to the direct optical transitions between the valence and conduction bands. Therefore, we expect to observe strong optical absorption lines at energies close to $E_{nlm}(\alpha)$. These will appear in the optical spectra at energies below the fundamental band gap. Absorption efficiency is defined by the oscillator strength (f_{cv}). For an "allowed" transition (s-exciton states only) the oscillator strength may be determined as [30,28]:

$$f_{cv}^{3D} = \frac{2\Omega_0}{\pi a_{\mathrm{B}}^3 m_0 E_{cv}} \frac{1}{n^3} \left|\langle c\,|\mathbf{ep}|\, v\rangle\right|^2; \qquad f_{cv}^{2D} = \frac{2a^2}{\pi a_{\mathrm{B}}^2 m_0 E_{cv}} \frac{1}{(n-1/2)^3} \left|\langle c\,|\mathbf{ep}|\, v\rangle\right|^2. \tag{22}$$

In addition, for a "forbidden" transition (p-exciton states only), the oscillator strength may be determined as [28]:

$$f_{cv}^{3D} = \frac{8\Omega_0 \beta_0^2}{3\pi a_{\mathrm{B}}^5 m_0 E_{cv}} \frac{n^2-1}{n^5} \left|\langle c\,|\mathbf{ep}|\, v\rangle\right|^2; \qquad f_{cv}^{2D} = \frac{8a^2\beta_0^2}{3\pi a_{\mathrm{B}}^4 m_0 E_{cv}} \frac{(n-1/2)^2 - 1}{(n-1/2)^5} \left|\langle c\,|\mathbf{ep}|\, v\rangle\right|^2, \tag{23}$$

where $\Omega_0 = a^2$c is the volume of unit cell, $\beta_0 = 3.0490$Å [6] is the distance between two nearest zinc atoms, $E_{cv} = \hbar\omega_{cv} = E_{nlm} - E_{vb}$ is the resonance photon energy (the difference between exciton E_{nlm} and valence E_{vb} energy levels), $|\langle c\,|\mathbf{ep}|\, v\rangle|$ – the optical matrix element.

5. Results and discussion

In our exciton energy calculations, the spin-orbit interaction was neglected. These assumptions allow us to consider the two exciton series that correspond to the heavy holes and light holes valence bands (hh, lh) and conduction band (c). Table 2 presents the main parameters of excitons, i.e. the relative effective mass (μ), the Bohr radius (a_{B}) and the parameter of anisotropy (α). It is noted that hh→c transition is characterized by maximal anisotropy ($|\alpha| \to 1$).

It is noteworthy that both anisotropy of the dispersion law plus the existence of crystalline packets (layers) normal to the main c-axis, will allow us to consider not only the volume $3D$-excitons but also two-dimensional $2D$-excitons thereto [30,28]. The display of high temperature phenomena caused by $2D$-excitons is not eliminated in these crystals. The calculated values of the binding energies (E_b) as well as the strength of oscillators for the optical transitions (f_{cv}) are given in tables 3, 4 both for a volume ($3D$) and for a plane ($2D$) excitons.

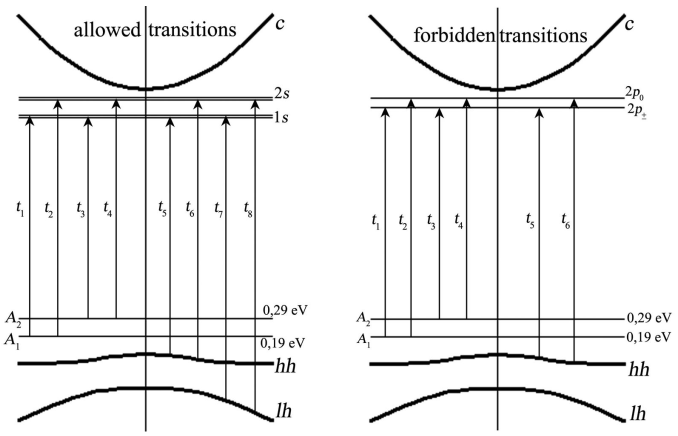

Figure 3. Schematic diagram of the localized level positions and transitions in Zn_3P_2.

Table 2. The main exciton parameters of Zn_3P_2.

Transition	$\mu_\perp/m_0$	$\mu_\parallel/m_0$	$a_{B\perp}$, Å	$a_{B\parallel}$, Å	α
hh→c	0.58	0.28	13.9	28.7	-1.04
lh→c	0.37	0.62	21.5	12.9	0.41

Table 3. Exciton binding energy.

exciton states	hh→c-bands, meV		lh→c-bands, meV	
	$3D$	$2D$	$3D$	$2D$
$1s$	26.2($\mathbf{e}_p \perp$c)	104.7($\mathbf{e}_p \perp$c)	25.8	103.3
$2s$	6.5($\mathbf{e}_p \perp$c)	11.6($\mathbf{e}_p \perp$c)	6.4	11.5
$2p_0$	5.3($\mathbf{e}_p \parallel$c)	9.5($\mathbf{e}_p \parallel$c)	—	—
$2p_\pm$	7.2($\mathbf{e}_p \parallel$c)	12.8($\mathbf{e}_p \parallel$c)	—	—

The data of tables 3, 4 show that the “allowed” transitions of an exciton with n=1 jointly provide the greatest contribution to optical effects. For the main exciton state, the binding energy is equal or exceeds the average heat motion energy ($k_0T \approx$ 25.8 meV) at room temperature. Therefore, the cutting peaks of the absorption or luminescence in the optical gap will be expected even at room temperature. This statement is also true for $2D$-exciton spectrum either in the bulk crystals or in the thin films and even with some strengthening.

A model of localized level positions and transitions in Zn_3P_2 determined by using our calculations is presented in figure 3. The energy-transition values listed in table 5 can be considered to be relatively well confirmed by data from different experiments.

Table 4. The optical transitions oscillator strength.

exciton states	hh→c-bands		lh→c-bands	
	$3D$	$2D$	$3D$	$2D$
$1s$	$3.6 \cdot 10^{-2}$	$3.7 \cdot 10^{-1}$	$2.4 \cdot 10^{-2}$	$3.8 \cdot 10^{-1}$
$2s$	$4.5 \cdot 10^{-3}$	$1.3 \cdot 10^{-2}$	$2.9 \cdot 10^{-3}$	$1.3 \cdot 10^{-2}$
$2p_0$	$2.1 \cdot 10^{-4}$	$4.6 \cdot 10^{-4}$	—	—
$2p_\pm$	$2.1 \cdot 10^{-4}$	$4.6 \cdot 10^{-4}$	—	—

Table 5. Energy values (in eV) of transition in Zn_3P_2 band structure.

	"allowed" transitions*	"forbidden" transitions*	all values from experiments**
t_1	1.38; 1.31	1.40; 1.39	1.23 PL [22]; 1.28 A [33];
t_2	1.40; 1.39	1.41; 1.40	1.31 P [21]; 1.32 A ($\mathbf{e}_p \parallel$c) [10];
t_3	1.28; 1.21	1.30; 1.29	1.34 P ($\mathbf{e}_p \parallel$c) [10];
t_4	1.30; 1.29	1.31; 1.30	1.36 A ($\mathbf{e}_p \perp$c) [10];
$A_1 \to$c	1.41	—	1.37 P ($\mathbf{e}_p \perp$c) [10]; 1.41 P [21];
$A_2 \to$c	1.31	—	1.44 PC [34]
t_5	1.57; 1.49	1.59; 1.58	1.46 A [10]; 1.52 R ($\mathbf{e}_p \parallel$c) [10];
t_6	1.59; 1.58	1.595; 1.59	1.54 R ($\mathbf{e}_p \perp$c) [10]; 1.55-1.60 A [11];
t_7	1.59; 1.51	—	1.59 A ($\mathbf{e}_p \perp$c) [5];
t_8	1.61; 1.60	—	1.59 R ($\mathbf{e}_p \perp$c) [5]; 1.60 PL [22];
hh→c	1.60 ($\mathbf{e}_p \perp$c)	1.60 ($\mathbf{e}_p \parallel$c)	1.60 PC ($\mathbf{e}_p \perp$c) [5]; 1.60 P [21];
lh→c	1.62	—	1.61 PC [34];1.62 A [5];1.63 PC,R [5]

*the first numeral is energy for $3D$ excitons; the second numeral is energy for $2D$ excitons.
**A, P, R, PL, PC denotes absorption, photovoltage, reflectivity, photoluminescence and photoconductive measurements, respectively.

6. Conclusions

Our calculations have shown a high binding energy of an exciton with $n = 1$. Moreover, it is noteworthy that both anisotropy of the dispersion law plus the existence of crystalline packets (layers) normal to the main optical axis, will make possible the existence of two-dimensional excitons too. So, the high temperature displaying of exciton effects is not eliminated even into bulk crystals. Comparison of available experimental data with our theoretical results testifies to an acceptable correlation between them. A series of optical experimental data from different sources may be simply and uniformly explained by using our calculations that are defined by $3D$ or $2D$-excitons. This provides some argumentation for the applied modelling approach as well as for all consequences following from that.

The offered model of energy transitions makes it possible to provide a simple explanation of many problem-solving situations, which were earlier explained by means of artificial suggestions about indirect band structure of Zn_3P_2. Under low temperature conditions, this model can be considered as a four-level scheme of the stimulated exciton radiation. The full process of exciton generation and annihilation can occur according to the scheme: v-band→ c-band→ exciton level→ acceptor or phonon oscillator level. The acceptor or phonon energy levels are par excellence occupied at a room temperature. However, at a low temperature these levels are loose. The automatic inversion of populating the upper and lower levels exists. Such a suggestion appears to be of interest both from practical and theoretical viewpoints and requires additional studies.

References

1. Andrzejewski J., Misiewicz J., Phys. Stat. Sol. B, 2001, **227**, No. 2, 515.
2. Hanuza J., Lemiec A., Misiewicz J., Vibrational Spectroscopy, 1998, **17**, 93.
3. Sieranski K., Szatkowski J., Misiewicz J., Phys. Rev., 1994, **50**, No. 11, 7331.
4. Weber A., Sutter P., von Kanel H., J. Appl. Phys., 1994, **75**, No. 11, 7448.
5. Misiewicz J., J. Phys.: Condens. Matter., 1990, **2**, 2053.
6. Zanin I.E., Aleinikova K.B., Afanasiev M.M., Antipin M.Yu., J. Struct. Chem., 2004, **45**, No. 4, 844.
7. Misiewicz J., J. Phys.: Condens. Matter., 1989, **1**, 9283.
8. Chuiko G., Dvornik O., Ivchenko V., Ukr. Phys. J., 2000, **45**, No. 10, 1188.
9. Pawlikowski J., Phys. Rev. B, 1982, **26**, No. 8, 4711.
10. Pawlikowski J., J. Appl. Phys., 1982, **53**, No. 5, 3639.
11. Fagen E.A., J. Appl. Phys., 1979, **50**, No. 10, 6505.
12. Misiewicz J., Bryja L., Jezierski K., et. al. Microelectronics J., 1994, **25**, XXIII.
13. Hava S., J. Appl. Phys., 1995, **78**, No. 4, 2808.
14. Pawlikowski J., Rev. Solid State Sci., 1989, **2**, 581.
15. Fessenden R., Sobhanadri J., Subramanian V., Thin Solid Films, 1995, **266**, 176.
16. Omari M., Kouklin N., Lu G, et. al., Nanotechnology, 2008, **19**, 105301.
17. Yang R., Chuen Y.-L., Morber J., et. al., Nano Lett., 2007, **7**, No 2, 269.
18. Shen G., Ye C., Goldberg D., Appl. Phys. Lett., 2007, **90**, 073115.
19. Zhao X.-G, Shi J.-L., Hu B., et. al., J. Mater. Chem., 2003, **13**, 399.
20. Green M., O'Brien P., J. Mater. Chem., 1999, **9**, 243.
21. Mirowska N., Misiewicz J., Semicond. Sci. Technol., 1992, **7**, 1332.
22. Nayak A., Rao D.R., Appl. Phys. Lett., 1993, **63**, No. 5, 592.
23. Arushanov E., Prog. Cryst. Growth Charact., 1992, **25**, 131.
24. Chuiko G., Don N., Ivchenko V., Functional Materials, 2005, **12**, No. 3, 454.
25. Chuiko G., Martyniuk V., Bazhenov V., Semicond. Phys. Quant. Electr. Optoelectr., 2004, **8**, No. 1, 28.
26. Chuiko G., Don N., Martyniuk V., Stepanchikov D., Semicond. Phys. Quant. Electr. Optoelectr., 2006, **9**, No. 2, 17.
27. Bychkov Yu.A., Rashba E.I., J.Phys.C.: Solid State Phys., 1984, **17**, 6039.
28. Knox R.S., Theory of excitons, Mir, Moscow, 1966 (in Russian).
29. Davidov A.S., Physics of solids, Nauka, Moscow, 1976 (in Russian).
30. Belenkii G.L., Stopachinsky V.B., UFN, 1983, **140**, No. 2, 233 (in Russian).
31. Vakarchuk I.O., Quantum mechanics, Lviv, 2004 (in Ukrainian).
32. Venger E., Pasechnik Yu., Shportko K., et. al., Visnyk Lviv. Univ. Ser. Phys., 2008, **41**, 28 (in Ukrainian).
33. Radautsan S., Syrbu N., Nebola I., Volodina V., Sov. Phys. Solid State, 1977, **19**, 1290.
34. Sobolev V., Syrbu N., Phys. Status Solidi B, 1974, **64**, 423.

Екситони в одновісних кристалах фосфіду цинку (Zn_3P_2)

Д.М.Степанчиков, Г.П.Чуйко

Херсонський національний технічний університет, кафедра загальної та прикладної фізики, науково-дослідна лабораторія теорії твердого тіла, Бериславське шосе, 24, 73008, Херсон, Україна

Отримано 18 травня 2008 р., в остаточному вигляді – 18 травня 2009 р.

Представлено теоретичне дослідження екситонних спектрів для кристалів $\mathrm{Zn_3P_2}$. Енергетичний спектр екситонів отримано у нульовому наближенні теорії збурень з урахуванням анізотропії закону дисперсії та правил відбору. Зафіксовано прояв двох серій екситонних станів, які відповідають двом валентним зонам (hh, lh) і зоні провідності (c). Гранична анізотропія закону дисперсії та шарувата кристалічна структура дозволяють очікувати на квазідвовимірний характер екситонів. Наслідком цього може стати високотемпературний прояв екситонних ефектів, навіть в об'ємних кристалах. Розраховано значення енергії зв'язку та сили осцилятора оптичного переходу для об'ємних ($3D$) і двовимірних ($2D$) екситонів. Запропоновано модель екситонних переходів і чотирирівневу схему стимульованого екситонного випромінювання для отримання лазерного ефекту.

Ключові слова: *екситони, фосфід цинку, одновісні кристали*

PACS: *71.18.+y*